International Journal of Hybrid Information Technology
Vol. 9, No.10 (2016), pp. 353-362
http://dx.doi.org/10.14257/ijhit.2016.9.10.34

Research of Comprehensive Compensation of Harmonics, Reactive current and DC Bias in UHV Power Grid

Baishan Zhao and Wenhui Li

School of Information Science and Engineering,
Shenyang University of Technology Shenyang, China
zhaobaishan@sut.edu.cn

Abstract

A comprehensive compensation device with paralleled decoupling for suppressing harmonics current, reactive power, and DC Bias of power transformer is proposed. Harmonics current and reactive current are detected by instantaneous reactive power theory. In this way, the fundamental active power is converted to be compensated reactive power and harmonics by controlling the converter. Compared to the ASVG with IGBT, the capacity and withstanding voltage level of ASVG with GTO are improved. The voltage across the devices of APF with multi-level inverter is reduced because of the paralleled decoupling connection. The harmonics compensation with multi-stage inverter can also reduce the voltage across the devices effectively. The reactive power compensator can work as a controllable rectifier and output controllable current by changing control algorithm. This current injects neutral point of transformer and suppresses its DC Bias, which has obvious effect on a power transformer. As a part of intelligent power grid, this compensator plays an important role for the development of smart grid automation.

***Keywords**: Parallel decoupling, harmonics, Reactive power, Multi-level inverter*

1. Introduction

The components of reactive power and harmonics current in power grid increase greatly because of using power electronic converters and other non-linear loads in recent years. At the same time, the transmission of AC with DC results in serious effects on the power transformer, including DC bias. They also affect the quality of electric energy, especially for the higher and higher voltage levels, which threatens the safe running of the UHV transmission system [1,2]. In order to transmit higher quality power, a comprehensive compensator is given to suppress the reactive power compensation, harmonic compensation and DC bias.

The harmonic components inside the power network lead to increase the additional loss and decrease the transmission efficiency. They can cause local overheat and increase vibration noise of transformer, which causes the pulsating torque of the motor and affect the normal operation of relay protection device and electric meter, even interfere with the communication system[3].

Reactive power in the power network not only increase the reactive power losses that drop the voltage of users, its mutation can also impact on the network and make the network unstable. The excitation current distortion caused by DC bias magnetic transformer makes the core supersaturated. It produces amount of harmonic and reactive power, so as to increase the vibration of the transformer noise and cause local overheating. As a result, it can shorten the life of transformer, even damages it [4,5].

The analysis above shows that the harmonic, reactive power and DC bias influence each others. DC magnetic bias of transformer produces a series of harmonics and reactive power, while the harmonic and the reactive power increase the vibration of the

ISSN: 1738-9968 IJHIT

transformer and loss, which weaken the bear ability of DC bias further. It is necessary to solute this problem by taking the three parameters as a whole.

The device consists of two parts: an inverter for reactive power compensation and DC bias suppression and a multistage inverter for the harmonic compensation[6]. Considering the higher required power of reactive power compensation and DC bias power inhibition as well as the lower switching frequency, the inverter circuit with Gate Turn-Off Thyristor (GTO) as switching device is taken as the main circuit for reactive power compensation and DC bias suppression device. Because of the higher withstand voltage of power grid, the paralleled decoupling and multistage inverter structure are used to overcome the lower withstand voltage of active power filter composed by Insulated Gate Bipolar Transistor (IGBT). The comprehensive compensation device proposed in this paper can operate safely in the UHV power grid. It guarantees the harmonic compensation in limited withstand voltage level of switch devices. It improves the capacity of reactive power compensator also and makes sure to inhibit the transformer DC bias.

The comprehensive compensation device for harmonic governance, reactive power compensation and DC bias suppression is verified by simulation in this paper. Compared with IGBT inverter, the inverter with GTO increases the capacity of overall system significantly. It can inhibit the DC bias of transformer effectively as the reactive power compensator under controllable rectifier condition. The switching device runs stably in higher voltage by using paralleled decoupling connection mode and multistage inverter to make the active filter with IGBT.

2. Topological Structure

Assuming the grid voltage is ideal undistorted voltage.

$$u_s(\mathrm{t})=\mathrm{U_s}\sin\omega\mathrm{t} \tag{1}$$

The load current i_L can be decomposed through Fourier transformation as following:

$$\begin{aligned} \mathrm{i_L(t)} &= \mathrm{I_1}\sin(\omega\mathrm{t}+\varphi_1)+\sum_{n=2}^{\infty} I_n \sin(n\omega\mathrm{t}+\varphi_n) \\ &= \mathrm{I_1}\sin\omega\mathrm{t}\cdot\cos\varphi_1+\mathrm{I_1}\cos\omega\mathrm{t}\cdot\sin\varphi_1+\sum_{n=2}^{\infty} I_n \sin(n\omega\mathrm{t}+\varphi_n) \\ &= i_{1p}(t)+i_{1q}(t)+i_h(t) \end{aligned} \tag{2}$$

Where $i_{1p}(t)$ is the fundamental component of active current, which forms the ideal current waveform. $i_{1q}(t)$ is the fundamental component of reactive current, which will be compensated by the reactive power compensation device. $i_h(t)$ is the harmonic component, which will be compensated by the active filter constructed with three multistage inverters [7].

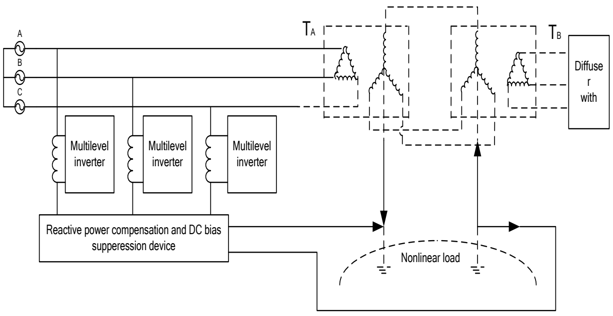

Figure 1. Schematic of Comprehensive Compensation Device

The schematic of the comprehensive compensation device is shown in Figure 1. Paralleled decoupling is used in the grid connection because both ends of the inverter are connected with the outputs of reactor in the reactive power compensation device, which reduces the terminal voltage of the active filter effectively. The three-phase active filter is constructed by three same single-phase multistage inverters, each structure of them is shown in Figure 2.

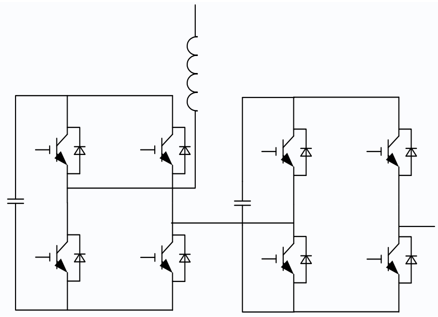

Figure 2. Configuration Diagram of Multi-Stage Inverter

It is shown in Figure 2 that the voltage is distributed averagely to each switch devices by multistage IGBT. The whole voltage level is improved, so the device can be used in UHV power grid for harmonic compensation.

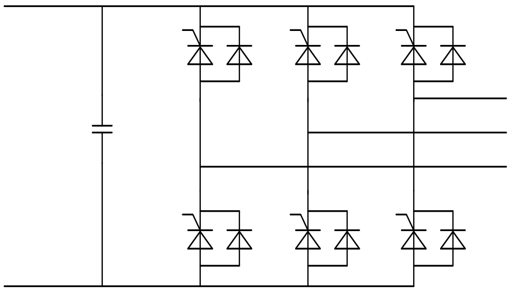

Figure 3. Device Structure of Reactive and DC Bias Compensation

The reactive power and DC bias compensation device is composed of three-phase bridge inverter circuit, as shown in Figure 3. Sensors combing with control chips determine to work in rectifier state for DC bias compensation or work in inverter state for reactive power compensation.

3. Mathematical Model

The schematic of the compensator is shown in Figure 4. Its equivalent circuit is shown in Figure 5.

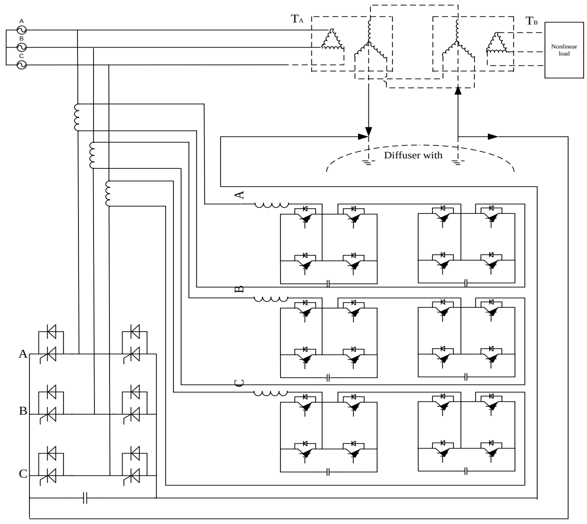

Figure 4. Overall Topology of the Compensation Device

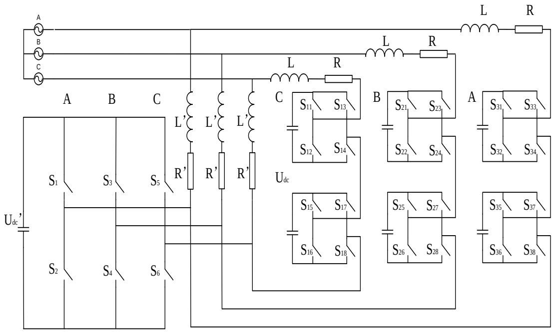

Figure 5. Equivalent Circuit

In Figure 4, the GTO and IGBT are equivalent to ideal switches, the switching losses are equivalent with *R*' and *R*, as shown in Figure 5. Ignoring the loss of IGBT, it can be taken as an ideal switch. U_{dc} is a constant and e_a, e_b, e_c are the grid voltages. The resistance and inductance of the transmission line are expressed respectively by *R* and *L*[8]. Take the neutral point of grid voltage as reference voltage. The voltage across the active filter is the voltage across *R′* and *L′*. According to the Kirchhoff's voltage law, the instantaneous voltage equation is obtained:

$$\begin{cases} u_A = Ri_A + L\dfrac{di_A}{dt} + u_{R'L'A} \\ u_B = Ri_B + L\dfrac{di_B}{dt} + u_{R'L'B} \\ u_C = Ri_C + L\dfrac{di_C}{dt} + u_{R'L'C} \end{cases} \tag{3}$$

The switching function S_A、S_B and S_C are:

$$S_K = \begin{cases} 1 & \text{the up branch on and the down branch off} \\ 0 & \text{the up branch off and the down branch on} \end{cases} \tag{4}$$

Taking phase A as an example, the states of switches corresponding respectively to the following: S_{11}, S_{14}, S_{15}, S_{18} on and S_{12}, S_{13}, S_{16}, S_{17} off express the up branch on and the down branch off; the up branch off and the down branch on in contrast.

K = A, B, C, in equation (4). The output phase voltage equation of the active filter is:

$$\begin{cases} u_A = u_{NO} + u_{AN} = u_{NO} + s_A u_{dc} \\ u_B = u_{NO} + u_{BN} = u_{NO} + s_B u_{dc} \\ u_C = u_{NO} + u_{CN} = u_{NO} + s_C u_{dc} \end{cases} \tag{5}$$

Because of the symmetrical of three-phase, we have

$$\begin{cases} i_A + i_B + i_C = 0 \\ u_A + u_B + u_C = 0 \end{cases} \tag{6}$$

According to the three formulas above, we have

$$u_{NO} = -\frac{1}{3}(S_A + S_B + S_C)u_{dc} \tag{7}$$

$$\begin{cases} u_A = (2S_A - S_B - S_C)u_{dc} \\ u_B = (-S_A + 2S_B - S_C)u_{dc} \\ u_C = (-S_A - S_B + 2S_C)u_{dc} \end{cases} \tag{8}$$

The mathematical model of multilevel inverter is obtained:

$$\begin{cases} L\frac{di_{cA}}{dt} = (\frac{2}{3}S_A - \frac{1}{3}S_B - \frac{1}{3}S_C)U_{dc} - (\frac{2}{3}S_A' - \frac{1}{3}S_B' - \frac{1}{3}S_C')U_{dc}' - Ri_{cA} + R'i_{cA}' \\ L\frac{di_{cB}}{dt} = (\frac{2}{3}S_B - \frac{1}{3}S_A - \frac{1}{3}S_C)U_{dc} - (\frac{2}{3}S_B' - \frac{1}{3}S_A' - \frac{1}{3}S_C')U_{dc}' - Ri_{cB} + R'i_{cB}' \\ L\frac{di_{cC}}{dt} = (\frac{2}{3}S_C - \frac{1}{3}S_B - \frac{1}{3}S_A)U_{dc} - (\frac{2}{3}S_C' - \frac{1}{3}S_B' - \frac{1}{3}S_A')U_{dc}' - Ri_{cC} + R'i_{cC}' \end{cases} \tag{9}$$

Similarly, the mathematical model of reactive power compensator is:

$$\begin{cases} L\frac{di_{cA}'}{dt} = (\frac{2}{3}S_A' - \frac{1}{3}S_B' - \frac{1}{3}S_C')U_{dc}' - R'i_{cA}' - e_A \\ L\frac{di_{cB}'}{dt} = (\frac{2}{3}S_B' - \frac{1}{3}S_A' - \frac{1}{3}S_C')U_{dc}' - R'i_{cB}' - e_B \\ L\frac{di_{cC}'}{dt} = (\frac{2}{3}S_C' - \frac{1}{3}S_B' - \frac{1}{3}S_A')U_{dc}' - R'i_{cC}' - e_C \end{cases} \tag{10}$$

The mathematical model of reactive power compensator for DC bias compensation is:

$$\begin{cases} L\frac{di_d}{dt} = -Ri_d + \omega Li_q + e_d - u_d \\ L\frac{di_q}{dt} = -Ri_q - \omega Li_d + e_q - u_q \\ C\frac{dU_{dc}}{dt} = \frac{3}{2}(S_d i_d + S_q i_q) - i_L \end{cases} \tag{11}$$

4. SVPWM Modulation Based on Voltage Space Vector

Any control system based on high frequency switching signal and power electronics needs a type of modulation. Traditional methods are PWM, SPWM, *etc*.[9][10]. In this paper, SVPWM modulation based on voltage space vector is used for the APF and the control algorithm of DC bias compensation devices. According to the equivalent circuit shown in Figure 5 and formula (8), the multistage inverter has eight kinds of output state, as shown in Table 1.

Table 1. Relationship of Switch State and APF's Output Phase Voltage

S_{abc}	u_a	u_b	u_c	$\boldsymbol{V_k}$
000	0	0	0	$\boldsymbol{V_0}$
100	2/3	-1/3	-1/3	$\boldsymbol{V_1}$
110	1/3	1/3	-2/3	$\boldsymbol{V_2}$

010	-1/3	2/3	-1/3	$\boldsymbol{V}_3$
011	-2/3	1/3	1/3	$\boldsymbol{V}_4$
001	-1/3	-1/3	2/3	$\boldsymbol{V}_5$
101	1/3	-2/3	1/3	$\boldsymbol{V}_6$
111	0	0	0	$\boldsymbol{V}_7$

APF output voltage vectors corresponding to switch mode are obtained from Table 1 as follow:

$$V_k = \begin{cases} \frac{2}{3} U_{dc}\, \mathrm{e}^{\mathrm{j}(k-1)\pi/3} & (k = 1, \cdots, 6) \\ 0 & (k = 0, 7) \end{cases} \tag{12}$$

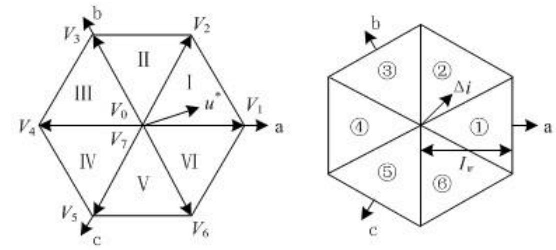

(a) Voltage vector diagram (b) Δi space area

Figure 6. Sector Partition

Eight switch states corresponding to the APF output voltage vector are in the area of a hexagon. The area is divided into six symmetrical triangles, as shown in Figure 6 (a). In order to reduce the difficulty of discriminating the positive and negative polarity of Δi_a, Δi_b and Δi_c, Δi space area is divided into six triangle area, noted as ①-⑥, hysteresis width is I_w, as shown in Figure 6(b).

The relationship between APF three-phase branches and switch signal can be seen from (12). To eliminate the influence among the phases, the space vectors are introduced, namely static $\alpha-\beta$ orthogonal coordinate system. When axis α overlap in axis β, the transformation relationship between the two coordinate systems is follow:

$$\begin{aligned} f &= f_\alpha + \mathrm{j}\, f_\beta \\ &= \frac{2}{3}(f_\mathrm{a} + f_\mathrm{b}\, \mathrm{e}^{\mathrm{j}2\pi/3} + f_\mathrm{c}\, \mathrm{e}^{\mathrm{j}4\pi/3}) \end{aligned} \tag{13}$$

Where f is current or voltage. By formula (13), the voltage vector equation of the multistage inverter is:

$$u = L\,\mathrm{d}i_c/\mathrm{d}t + Ri_c + u_{R'L'} \tag{14}$$

When the output current is instruction current vector $\boldsymbol{i}_c^*$, we have:

$$u^* = L\,\mathrm{d}i_c^*/\mathrm{d}t + Ri_c^* + u_{R'L'} \tag{15}$$

u^* in (15) is the output reference voltage vector of APF corresponding with instruction current vector i_c^*. Define

$$\Delta i = i_c^* - i_c \tag{16}$$

Subtracting (14) from (15) and ignoring the APF AC side resistance, there is

$$L\,\mathrm{d}\Delta i/\mathrm{d}t = u^* - u \tag{17}$$

Formula (17) shows that the change rate of current error vector Δi is dependent on the deference between reference voltage vector u^* and voltage deviation of APF output voltage vector u. For a given reference voltage vector u^*, APF output voltage vector vitamin $V_k(k=0,\ldots,7)$ can be chosen appropriately to control the rate $d\Delta i/dt$ of the current error vector Δi, so that control the current error vectorΔi.

5. Simulation Results Analysis

The topology structure and mathematical model above are simulated by Simulink. The compensation ability on reactive power, harmonic and transformer DC bias by this device is analyzed. The simulation results are shown in Figure 7, including the distribution network, transmission line, and various nonlinear load detection, conversion device. The APF uses DC to AC conversion circuit. The IGBT in the inverter on or off, the modulation mode of control system based on voltage space vector SVPWM and the control strategy of instantaneous reactive power of non harmonic current detection based control system are controlled by six channel control signals. Power System Blockset of simulink provides the measurement unit, transformer, rectifier and load in Figure 7. The main transformation module, flux torque observation module, sector, switch selection module are built according to the principle of self-built combination module.

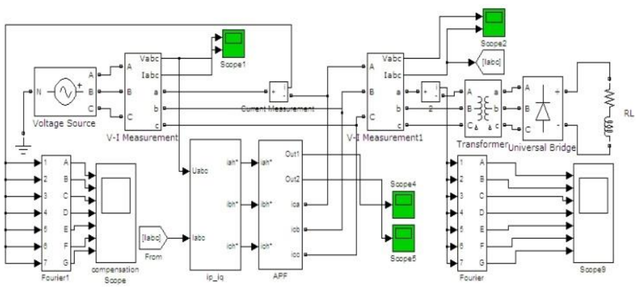

Figure 7. APF Simulation Diagram

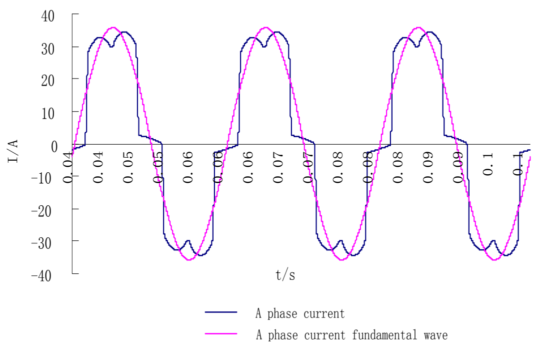

Figure 8. Phase a Current Fundamental and Harmonic Compared

The phase A grid current and phase A current with harmonics are shown in Figure 8. APF is the plot of instruction current and tracking current in Figure 9. The phase A current of before and after APF compensation is shown in Figure 10. It shows that the compensation effect is obviously. It can be seen from Figure 11 that the 5, 7 and 11 harmonic components decrease significantly after compensation. The harmonic components of transformer excitation current are also reduced obviously after the DC bias compensation, as shown in Figure 12.

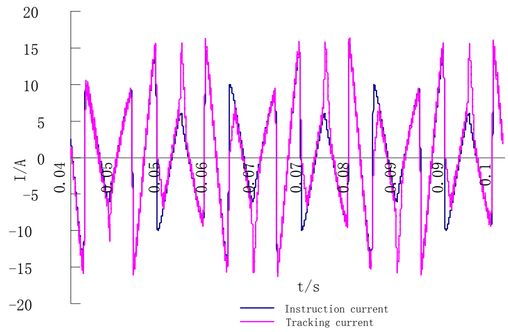

Figure 9. APF Instruction Current and Tracking Current

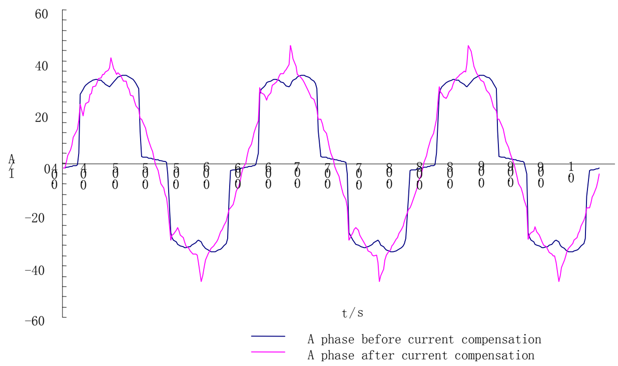

Figure 10. Phase a Current before and After APF

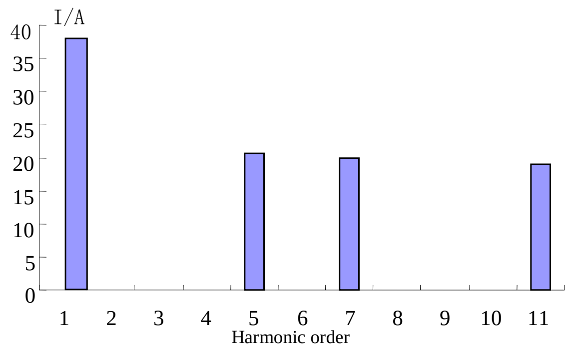

a) Harmonic current before filtering

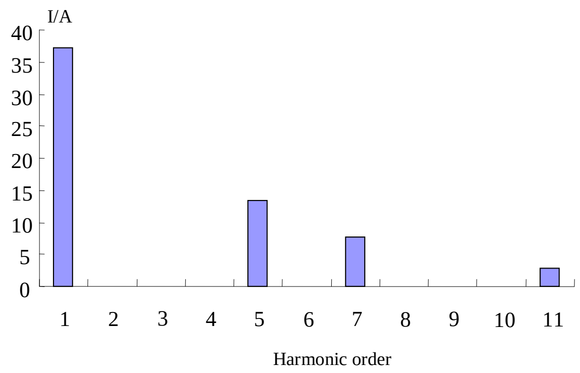

b) Harmonic current after filtering

Figure 11. Phase a Current Spectrum Analysis

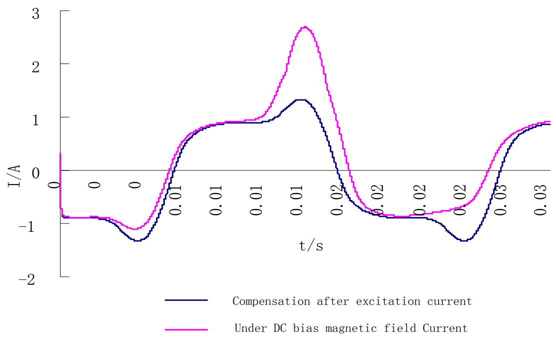

Figure 12. Excitation Current Waveform Before and After DC Bias Compensation

6. Conclusion

From the analysis above and contracting the APF with multistage inverter to ordinary three-phase bridge circuit structure, we can know that the former has higher withstanding voltage levels and more capacity. Combining reactive power compensation device constructed by GTO with APF constructed by IGBT relieve the inadequate capacity greatly of the APF in reactive power compensation. The simulation results show that this device have good properties on reactive power compensation, harmonic governance and DC bias suppression in UHV power grid.

Acknowledgements

This work was supported by Ministry of Education Key Project of Science and Technology of China (No.211037) and the general scientific research project of the Education Department of Liaoning Province, China (No.L2014053).

References

[1] L. C. David and H. Li, "An improved adaptive detection method for power quality improvement", Conference Record of the 2006 IEEE Industry Applications Conference Forty First ISA Annual Meeting, TAMPA, FL, USA, **(2006)**.
[2] G. Manchur and C. C. Erven, "Development of a model for predicting flicker from electric arc furnaces", IEEE Transactions on Power Delivery, vol. 7, no. 1, **(1992)**.
[3] M. Jiang, X. Wang, J. Lou, J. He and T. Yip, "Analysis and prediction of harmonic current in feeder of traction substation", Power System Technology, vol. 38, no. 1, **(2014)**.
[4] H. Leopold, P. Igor and B. Bostjan, "A proportional-resonant current controller for selective harmonic compensation in a hybrid active power filter", IEEE Transactions on Power Delivery, vol. 29, no. 5, **(2014)**.
[5] W. Sima,Y. Zhou, T. Yuan, Q. Yang, S. Sun and G. Tremouille, "Analysis on phase arrangement and transposition modes for UHV DC and double-circuit EHV AC transmission line built on the same tower", High Voltage Engineering, vol. 38, no. 12, **(2012)**.
[6] B. Aziz and B. Tahar, "Fuzzy logic controlled shunt active power filter for harmonic compensation and power quality improvement", Journal of Engineering Science and Technology Review, vol. 7, no. 4 **(2014)**.
[7] L. Qian, C. David and Q. Zhang, "Three-phase harmonic selective active filter using multiple adaptive feed forward cancellation method", IEEE 5th International Power Electronics and Motion Control Conference Shanghai,China, **(2006)**.
[8] X. Cui, "An improved ip-iq harmonic detection algorithm", Advanced Materials Research, **(2012)**, pp. 588-589.
[9] Y. Wang, N. Gao, Y. Luo and X. Cai, "SPWM Research for Dead-time Elimination in a Three-phase Three-level Grid-connected Inverter", Proceedings of the Chinese Society for Electrical Engineering, vol. 31, no. 21, **(2011)**.
[10] A. R. Beig, "Synchronized SVPWM algorithm for the overmodulation region of a low switching frequency medium-voltage three-level VSI", IEEE Transactions on Industrial Electronics, vol. 59, no. 12, **(2012)**.

Authors

Baishan Zhao, he is a Doctor, working in Shenyang University of Technology, China, devoting to the research of digital signal processing.

Wenhui Li, she is a Master, studying in the Shenyang University of Technology, China, engaging in harmonic signal suppression for power transmission network.